MULTI-OBJECTIVE OPTIMIZATION DESIGN OF CRANK TRIANGULAR LINKAGE-ELBOW MECHANISM BASED ON ANALYTICAL HIERARCHY PROCESS METHOD

Minhai MA[1, 2], Tao LV[1, 2*]

In response to the various parameter requirements of the crank triangular linkage-elbow mechanism of a certain model of servo press, the kinematic analysis of the crank triangle elbow mechanism is first carried out using the complex vector method. Then based on design variables and constraints, the basic dimensions of the transmission mechanism in MATLAB (Matrix Laboratory) are calculated. The design variables, constraints, and objective function are identified. Third, 6 design variables and 15 constraint conditions are selected to minimize the error between the optimized slider velocity curve and the target curve, and maximize the acceleration of the slider, and the stroke ratio coefficient as the objective functions. Finally, the AHP (Analytic Hierarchy Process) method is used to determine the weight coefficients of the linear weighted sum method. Combined with the penalty function method, the GA (Genetic Algorithm) is used to calculate the final objective function value. The research results indicate that the optimized crank triangular linkage-elbow mechanism meets the working performance requirements of enterprises.

Keywords: Servo press; crank triangular linkage-elbow mechanism; multi-objective optimization design; AHP

1. Introduction

In recent years, AC servo drive technology has made rapid development and gradually applied to the field of traditional mechanical presses, developing into servo presses [1]. Servo presses not only maintain the various advantages of traditional mechanical presses, but also overcome the disadvantages of difficult adjustment of working characteristics. Servo presses have the characteristics of intelligent and flexible processing, greatly improving process adaptability. In addition, servo presses have the characteristics of simple structure, convenient installation and maintenance, low energy consumption, and light weight. According to the requirements of the stamping process, the transmission mechanism of the servo presses should have the characteristics of pressure

[1]Precision Mold Processing and Intelligent Manufacturing Research Center, Ningbo Polytechnic, 288 Lushan Road, Ningbo, 315800, China
[2]Department of Mechanical Engineering and Mechanics, Ningbo University, 818 Fenghua Road, Ningbo, 315211, China
[*]Corresponding author: Associate professor, Email: tomtaolv@163.com

retaining performance and fast return. Therefore, the optimization design of servo press transmission mechanism has always been one of the hotspots in this field [2].

Many researches have been conducted on the optimization design of servo presses transmission mechanisms by using different methods. Peón-Escalante et al. [3] proposed a composite formula that uses a dual function and finite difference to calculate the output chain. Numerical comparisons were made between the velocity and acceleration coefficients of the output link, and the results showed the accuracy of the formula. Finally, the optimal size synthesis of the Stephenson III six bar mechanism was presented. Qaiyum and Mohammad [4] proposed a design method for a six bar mechanism with rotating joints. This method obtains the optimal solution of the six bar mechanism by designing a mathematical model composed of two vector closed-loop equations and using PSO(Particle Swarm Optimization) optimization algorithm. Finally, the final design parameters and convergence speed of the optimal solution were given. Belleri and Kerur [5] proposed an optimization design method for the balance of planar six bar mechanisms. This method can solve the optimization problem by designing an objective function, and GA and MATLAB software can be used to minimize fluctuations in vibration force and torque. Among them, the selection of weighting factors plays a crucial role in obtaining the optimal values of design parameters. Through setting two sets of weighting factors and comparing them with the original values, the optimized vibration force and torque were significantly reduced. Reza and Moslehi [6] proposed a design method for size synthesis of adjusTable six bar mechanisms using the COA (Cuckoo Bird Optimization Algorithm). The path generated by the size optimization of the four bar mechanism was compared with the obtained results, demonstrating the superior performance of COA. After obtaining the optimal size of the four-bar mechanism, an adjusTable six bar mechanism was obtained through re-optimization of the mechanism. The results indicate that compared with the four bar mechanism, the adjusTable six bar mechanism can obtain a more accurate path. Sanchez-Marin, and Roda-Casanova [7] developed a complete method for searching for high-quality six bar mechanisms. This method is used to explore the design space to search for optimal stopping link and determine the type of link that provides optimal stopping based on established standards. Then, evolutionary algorithms are used for global optimal search. The results demonstrate the efficiency and versatility of this method. Yazdani and Abyaneh [8] provided six bar mechanism design method based on GA. They defined an objective function for the slider. The function of the speed slider is to use a mathematical relationship with the kinematic constraints of the mechanism. The genetic algorithm is used for optimization design. The experimental results show that this method can provide an optimal solution for the size of a six bar mechanism.

Some of the above methods are prone to falling into local optima, while others remain in theoretical calculations and are not practical in actual design. The AHP method is used here to solve the weight coefficient problem, and the linear weighted sum method and genetic algorithm are used to achieve the global optimal solution [9]. The experimental results show that this method has strong practicality due to its consideration of engineering practice.

2. Research method

2.1 Kinematic analysis of crank triangular linkage-elbow mechanism

2.1.1. Crank triangular linkage-elbow mechanism

Figure 1 shows the crank triangular linkage-elbow mechanism of a servo press. l_1 is the crank; l_2, l_4, and l_5 form a triangular toggle linkage; l_3 is the upper link; l_6 is the lower link, and s is the slider. θ_1, θ_2, θ_3, θ_4, θ_5 and θ_6 is the azimuth angle of each rod. A is the hinge point between the crank and the frame; B is the hinge point between the crank and the triangular linkage-elbow; C is the hinge point between the upper link and the frame; D is the hinge point between the upper link and the triangular linkage-elbow; E is the hinge point between the lower link and the triangular linkage-elbow, and F is the hinge point between the lower link and the slider. Taking A as the origin, x and y are the horizontal and vertical coordinates of E in the frame. h is the distance from the center of the slider to point C. ω_1 and ε_1 are the angular velocity and angular acceleration of the crank, respectively, $l_i\,(i=1,2,3,4,5,6)$, and $\theta_1, \omega_1, \varepsilon_1, x$, and y are known conditions.

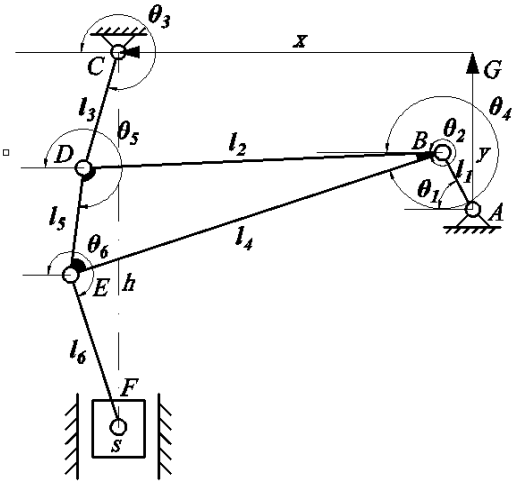

Fig. 1 Crank triangular linkage-elbow mechanism

2.1.2 Analysis of position of the slider

The complex vector method is used for kinematic analysis of the crank triangular linkage-elbow mechanism [10]. $\vec{l}_1$ is the vector of rod 1, and the rest of rods in the mechanism can be represented in this way. The closed graph composed of each rod vector is called a closed vector polygon, in which the sum of the vectors should be equal to zero. The vector equation of the mechanism can be obtained from the closed polygon ABDCG as follows:

$$\vec{l}_1 + \vec{l}_2 - \vec{l}_3 - \vec{x} - \vec{y} = 0 \tag{1}$$

Eq. (1) is rewritten into the plural form:

$$l_1 e^{i\theta_1} + l_2 e^{i\theta_2} = x + yi + l_3 e^{i\theta_3} \tag{2}$$

Using the Euler formula $e^{i\theta} = \cos\theta + i\sin\theta$, the real part and imaginary part of Eq. (2) are distinguished, and two equations are obtained as follows:

$$l_1 \cos\theta_1 + l_2 \cos\theta_2 = x + l_3 \cos\theta_3 \tag{3}$$

$$l_1 \sin\theta_1 + l_2 \sin\theta_2 = y + l_3 \sin\theta_3 \tag{4}$$

Simplify Eqs. (3) and (4):

$$A\sin\theta_2 + B\sin\theta_2 + C = 0 \tag{5}$$

where $A = 2l_1 l_2 \sin\theta_1 - 2yl_2$, $B = 2l_1 l_2 \cos\theta_1 - 2xl_2$, and $C = l_1^2 + l_2^2 + x^2 + y^2 - l_3^2 - 2xl_1\cos\theta_1 - 2yl_1\sin\theta_1$

After using the trigonometric function formula, Eq. (5) can be transformed into:

$$2A\sin\frac{\theta_2}{2}\cos\frac{\theta_2}{2} + B\left(\cos^2\frac{\theta_2}{2} - \sin^2\frac{\theta_2}{2}\right) + C\left(\cos^2\frac{\theta_2}{2} + \sin^2\frac{\theta_2}{2}\right) = 0 \tag{6}$$

Both sides of the equation are divided by $\cos^2\frac{\theta_2}{2}$ at the same time, and then after sorting:

$$\tan\frac{\theta_2}{2} = \frac{A - \sqrt{A^2 + B^2 - C^2}}{B - C} \tag{7}$$

$$\theta_2 = 2\arctan\frac{A - \sqrt{A^2 + B^2 - C^2}}{B - C} \tag{8}$$

Substituting θ_2 into Eqs. (3) and (4), it can be obtained that:

$$\theta_3 = \arctan\frac{l_1\sin\theta_1 + l_2\sin\theta_2 - y}{l_1\cos\theta_1 + l_2\cos\theta_2 - x} \tag{9}$$

The vector equation of the mechanism obtained from the closed polygon BDE is:

$$\vec{l_2} + \vec{l_5} = \vec{l_4} \tag{10}$$

Similarly, from the above methods, it can be concluded that:

$$\theta_5 = 2\arctan\frac{D - \sqrt{D^2 + E^2 - F^2}}{E - F} \tag{11}$$

$$\theta_4 = \arccos\frac{l_2\cos\theta_2 + l_5\cos\theta_5}{l_4} \tag{12}$$

where $D = 2l_2l_5\sin\theta_2$, $E = 2l_2l_5\cos\theta_2$, and $F = l_1^2 + l_5^2 - l_4^2$

The vector equation of the mechanism obtained from the closed polygon CDEF is:

$$\vec{l_3} + \vec{l_5} + \vec{l_6} = \vec{h} \tag{13}$$

Similarly, from the above methods, it can be concluded that:

$$\theta_6 = \arccos\left(\frac{-l_3\cos\theta_3 - l_5\cos\theta_5}{l_6}\right) \tag{14}$$

$$h = -l_3\sin\theta_3 - l_5\sin\theta_5 - l_6\sin\theta_6 \tag{15}$$

2.1.3. Analysis of speed and acceleration of the slider

The first derivative of Eqs. (3) and (4) is found with respect to time to obtain Eqs. (16) and (17), where ω_i represents the angular velocity of each rod, and V_7 represents the velocity of the slider.

$$l_1\omega_1\sin\theta_1 + l_2\omega_2\sin\theta_2 = l_3\omega_3\sin\theta_3 \tag{16}$$

$$l_1\omega_1\cos\theta_1 + l_2\omega_2\cos\theta_2 = l_3\omega_3\cos\theta_3 \tag{17}$$

Thus, the angular velocity equation can be obtained:

$$\omega_2 = \frac{l_1\omega_1\sin(\theta_1 - \theta_3)}{l_2\sin(\theta_3 - \theta_2)} \tag{18}$$

$$\omega_3 = \frac{l_1\omega_1\sin(\theta_2 - \theta_1)}{l_3\sin(\theta_2 - \theta_3)} \tag{19}$$

Using the same method, the velocity of each rod and slider can be obtained:

$$\begin{cases} \omega_2 = \dfrac{l_1\omega_1 \sin(\theta_1 - \theta_3)}{l_2 \sin(\theta_3 - \theta_2)} \\ \omega_3 = \dfrac{l_1\omega_1 \sin(\theta_2 - \theta_1)}{l_3 \sin(\theta_2 - \theta_3)} \\ \omega_4 = \dfrac{l_2\omega_2 \sin\theta_2 + l_5\omega_5 \sin\theta_5}{l_4 \sin\theta_4} \\ \omega_5 = \dfrac{l_2\omega_2 \sin(\theta_4 - \theta_2)}{l_5 \sin(\theta_5 - \theta_4)} \\ \omega_6 = -\dfrac{l_3\omega_3 \sin\theta_3 + l_5\omega_5 \sin\theta_5}{l_6 \sin\theta_6} \\ V_7 = -l_3\omega_3 \cos\theta_3 - l_5\omega_5 \cos\theta_5 - l_6\omega_6 \cos\theta_6 \end{cases} \tag{20}$$

The second derivative of Eqs. (3) and (4) are found with respect to time to obtain Eqs. (21) and (22), in which ε_i represents the angular acceleration of each rod, and a_7 represents the acceleration of the slider.

$$l_1\varepsilon_1 \sin\theta_1 + l_1\omega_1^2 \cos\theta_1 + l_2\varepsilon_2 \sin\theta_2 + l_2\omega_2^2 \cos\theta_2 = l_3\varepsilon_3 \sin\theta_3 + l_3\omega_3^2 \cos\theta_3 \tag{21}$$

$$l_1\varepsilon_1 \cos\theta_1 - l_1\omega_1^2 \sin\theta_1 + l_2\varepsilon_2 \cos\theta_2 - l_2\omega_2^2 \sin\theta_2 = l_3\varepsilon_3 \cos\theta_3 - l_3\omega_3^2 \sin\theta_3 \tag{22}$$

Thus, the angular acceleration equation can be obtained as follows:

$$\varepsilon_2 = \frac{l_1\varepsilon_1 \sin(\theta_1 - \theta_3) + l_1\omega_1^2 \cos(\theta_1 - \theta_3) + l_2\omega_2^2 \cos(\theta_2 - \theta_3) - l_3\omega_3^2}{l_2 \sin(\theta_3 - \theta_2)} \tag{23}$$

$$\varepsilon_3 = \frac{l_1\varepsilon_1 \sin\theta_1 + l_1\omega_1^2 \cos\theta_1 + l_2\varepsilon_2 \sin\theta_2 + l_2\omega_2^2 \cos\theta_2 - l_3\omega_3^2 \cos\theta_3}{l_3 \sin\theta_3} \tag{24}$$

Using the same method, the acceleration of each rod and slider can be obtained:

$$\begin{cases} \varepsilon_2 = \dfrac{l_1\varepsilon_1 \sin(\theta_1-\theta_3)+l_1\omega_1^2 \cos(\theta_1-\theta_3)+l_2\omega_2^2 \cos(\theta_2-\theta_3)-l_3\omega_3^2}{l_2 \sin(\theta_3-\theta_2)} \\ \varepsilon_3 = \dfrac{l_1\varepsilon_1 \sin\theta_1+l_1\omega_1^2 \cos\theta_1+l_2\varepsilon_2 \sin\theta_2+l_2\omega_2^2 \cos\theta_2-l_3\omega_3^2 \cos\theta_3}{l_3 \sin\theta_3} \\ \varepsilon_4 = \dfrac{l_2\varepsilon_2 \sin\theta_2+l_2\omega_2^2 \cos\theta_2+l_3\varepsilon_3 \sin\theta_3+l_3\omega_3^2 \cos\theta_3-l_4\omega_4^2 \cos\theta_4}{l_4 \sin\theta_4} \\ \varepsilon_5 = \dfrac{l_2\varepsilon_2 \sin(\theta_4-\theta_2)-l_2\omega_2^2 \cos(\theta_2-\theta_4)-l_5\omega_5^2 \cos(\theta_3-\theta_4)+l_4\omega_4^2}{l_3 \sin(\theta_5-\theta_4)} \\ \varepsilon_6 = \dfrac{l_6\omega_6^2 \cos\theta_6-l_3\varepsilon_3 \sin\theta_3-l_3\omega_3^2 \cos\theta_3-l_5\varepsilon_5 \sin\theta_5-l_5\omega_5^2 \cos\theta_5}{l_6 \sin\theta_6} \\ a_7 = l_3\omega_3^2 \sin\theta_3-l_3\varepsilon_3 \cos\theta_3+l_5\omega_5^2 \sin\theta_5-l_5\varepsilon_5 \cos\theta_5+l_6\omega_6^2 \sin\theta_6-l_6\varepsilon_6 \cos\theta_6 \end{cases} \tag{25}$$

2.2. Simulation analysis of crank triangular linkage-elbow mechanism

ADAMS (Automatic Dynamic Analysis of Mechanical Systems) is virtual prototype development system software based on computational multibody system dynamics and integrates modeling, calculation, solution, post-processing, and visualization technologies. It includes multiple professional modules and serves multiple specialized fields [11]. The View module and Postprocess module are the basic modules in ADAMS, suitable for common mechanical system problems. They are used for kinematic analysis of the servo press. ADAMS also has independently developed modules and embedded modules for certain professional fields [12]. It has rich and powerful functions. Starting from the early stage of product research, it can avoid repetitive manufacturing of physical prototypes, save development costs, improve efficiency, and have a clear software interface, simple operation, and convenient modification. Its problem-solving ability has been verified by a large number of practical engineering problems. It is a professional dynamic software that has been tested in industry.

A in Fig. 1 is taken as the coordinate origin, and the basic dimension data of the crank triangular linkage-elbow mechanism involved is shown in Table 1.

Table 1

Basic dimensions of the crank triangular linkage-elbow mechanism

Items	Value
l_1 (mm)	229.2
l_2 (mm)	788
l_4 (mm)	893
l_5 (mm)	340
l_3 (mm)	290
l_6 (mm)	430
x (mm)	680
y (mm)	160

Based on the basic dimensions of the mechanism, a kinematic simulation model (slider stroke, velocity, acceleration) of the crank triangular linkage-elbow mechanism is established in ADAMS. According to the requirements of stamping, processing should be carried out in the range of the process stroke. The slider stroke, slider speed, slider acceleration, and stroke speed ratio coefficient should meet certain requirements.

Figure 2 shows the kinematic curve of the initial slider. The horizontal axis represents the crank rotation angle θ_1, while the vertical axis represents the slider stroke $l_3 + l_5 + l_6 - h$, velocity V_7, and acceleration a_7, respectively. Table 2 shows the initial value and improvement requirements. Combined with Figure 2 and Table 2, it can be seen that the green line represents the stamping process stroke (i.e. crank angle 323 °~341 °). The initial design plan is within the stamping process stroke, and the speed and fluctuation of the slider significantly exceed the processing requirements, which can easily cause cracking of the part during the stretching process. Therefore, it is necessary to optimize and adjust the design parameters.

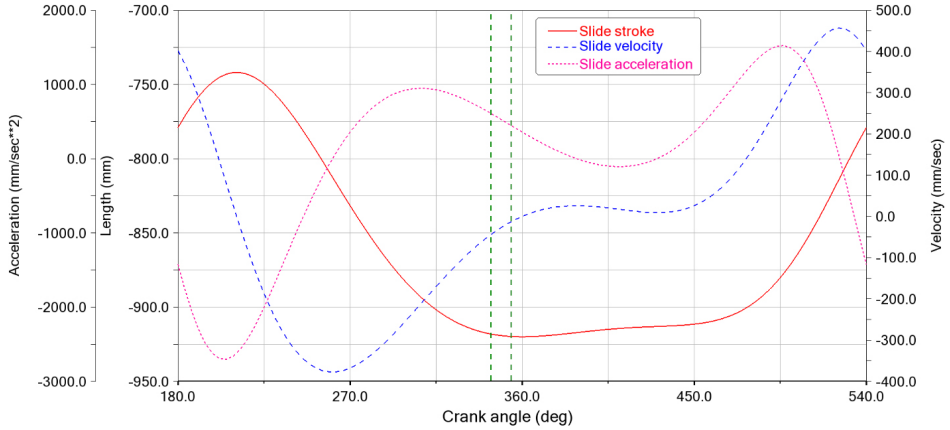

Fig. 2. Initial slider kinematic curve

Table 2

Initial value and improvement needs

Parameters	Initial value	Improvement needs
Slider stroke(mm)	181	>175
Slider velocity(mm/s)	-37.5~-16.5	-30,Keep it as constant as possible
Slider acceleration(mm/s^2)	685.8~524.4	As small as possible
Stroke speed ratio coefficient	0.92	>1.4

2.3. Multi-objective optimization design

2.3.1. Design variable

There are two types of parameters in the optimization design, namely design constants and design variables. The fixed and unchanging parameters are design constants, and the independent parameters that need to be adjusted appropriately are design variables [13]. The selection of design variables affects the complexity of optimization design. In n dimensional optimization problems, the number of design variables determines the degree of freedom (DOF) in the optimization process. The larger the DOF, the more ideal the optimization result will be, but the complexity will correspondingly increase. Reducing the design variables as much as possible without affecting the performance of the transmission system is beneficial for reducing the difficulty of optimizing the size of the mechanism [14]. As shown in Figure 1, when l_1, x, and y is determined, l_2, and l_4 is also determined accordingly. The design variables for this article are $X=[l_1,l_3,l_5,l_6,x,y]$.

2.3.2. Constraint condition

Figure 3 shows a crank rocker mechanism composed of l_1, l_2, l_3 and $\sqrt{x^2+y^2}$, and it should meet the conditions of a crank, that is, the crank is the shortest and the sum of the lengths of the crank and any rod is less than the sum of the lengths of the other two rods [15]. The constraint expression is as follows:

$$g_1(X) = l_1 + l_2 - l_3 - \sqrt{x^2+y^2} \le 0 \tag{26}$$

$$g_2(X) = l_1 + l_3 - l_2 - \sqrt{x^2+y^2} \le 0 \tag{27}$$

$$g_3(X) = l_1 + \sqrt{x^2+y^2} - l_2 - l_3 \le 0 \tag{28}$$

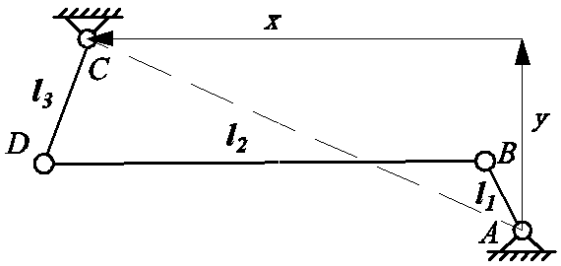

Fig. 3 Crank-rocker mechanism

According to the size range provided by the enterprise, the constraint conditions can be determined:

$$\begin{cases} g_4(X) = l_1 - 220 \le 0 \\ g_5(X) = 100 - l_1 \le 0 \\ g_6(X) = l_3 - 350 \le 0 \\ g_7(X) = 250 - l_3 \le 0 \\ g_8(X) = l_5 - 500 \le 0 \\ g_9(X) = 300 - l_5 \le 0 \\ g_{10}(X) = l_6 - 500 \le 0 \\ g_{11}(X) = 300 - l_6 \le 0 \\ g_{12}(X) = x - 800 \le 0 \\ g_{13}(X) = 400 - x \le 0 \\ g_{14}(X) = y - 300 \le 0 \\ g_{15}(X) = 50 - y \le 0 \end{cases} \tag{29}$$

2.3.3. Objective function

(1) Objective function of the slider velocity

The noise generated by sheet metal stamping is the greatest, and the main part of stamping noise is the moment when the material is cut off. The collision between the punch and slider causes the sudden release of elastic deformation energy accumulated in the press body, resulting in shock vibration and radiation of strong noise. Therefore, this article will determine reducing the maximum speed of the transmission mechanism slider as the first optimization objective:

$$f_1(X) = \min\left(\left|v(x)_{\max}\right|\right) \tag{30}$$

where $\left|v(x)_{\max}\right|$ represents the maximum velocity of the slider in the important machining stroke.

(2) Objective function of slider acceleration

During high-speed motion, the inertial force generated by the slider increases the load on the servo motor and affects the machining accuracy of the press. The weight and acceleration of the slider in the transmission mechanism are two main factors that generate inertial force. This article determines reducing the maximum acceleration of the slider in the transmission mechanism as the second optimization objective:

$$f_2(X) = \min\left(\left|a(x)\right|_{\max}\right) \tag{31}$$

where $\left|\mathrm{a}(x)_{\max}\right|$ represents the maximum acceleration of the slider in the important machining stroke.

(3) Objective function of travel speed ratio coefficient

To maximize the travel speed ratio coefficient of the crank triangle elbow mechanism, improve work efficiency, save power, and meet the characteristics of quick return, according to the travel speed ratio coefficient requirements proposed by the enterprise, the travel speed ratio coefficient is set as the third goal.

$$f_3(X) = \max(K), K > 1.4 \tag{32}$$

2.4. Multi-objective optimization calculation method

2.4.1. Optimization objective function

For single objective optimization design problems, the optimal solution can be easily obtained within its constraints. However, multi-objective optimization design problems have significant differences. The optimization of each sub-objective in multi-objective optimization design problems often contradicts each other, and the resulting solution is often the optimal solution of one sub-objective that cannot meet the optimization of other sub-objectives. It is

difficult to determine the quality of its solution, and multi-objective optimization design problems generally have many optimal solutions, making it difficult to obtain the optimal solution [16].

The linear weighted sum method is selected to analyze the multi-objective optimization design problem of the crank triangle elbow mechanism. The principle of the linear weighted sum method is to give appropriate weight coefficients to each sub-objective based on the importance of each sub-objective [17]. Then, the sub-objective functions are multiplied by their own weight coefficients and added together to form the following final evaluation function:

$$f(X)=W_1 f_1(X)+W_2 f_2(X)+W_3 f_3(X) \tag{33}$$

where W_1 , W_2 ,and W_3 are the weight coefficients of each sub-objective. $\sum_{i=1}^{3} W_i = 1$, and $W_i \geq 0$.

2.4.2. AHP (Analytical Hierarchy Process)

The weight coefficients of the linear weighted sum method are often determined by the experience of designers, which makes the design results highly subjective. The AHP is selected to determine the weight coefficients. AHP refers to the process of treating a complex multi-objective decision-making problem as a system, decomposing the objective into multiple objectives or criteria, and then decomposing them into multiple levels of multiple indicators. Using qualitative indicator fuzzy quantification methods, the hierarchical single ranking and total ranking are calculated, serving as a systematic method for objective optimization decision-making [18]. The standard process of AHP is shown in Figure 4. The hierarchical structure model is shown in Figure 5.

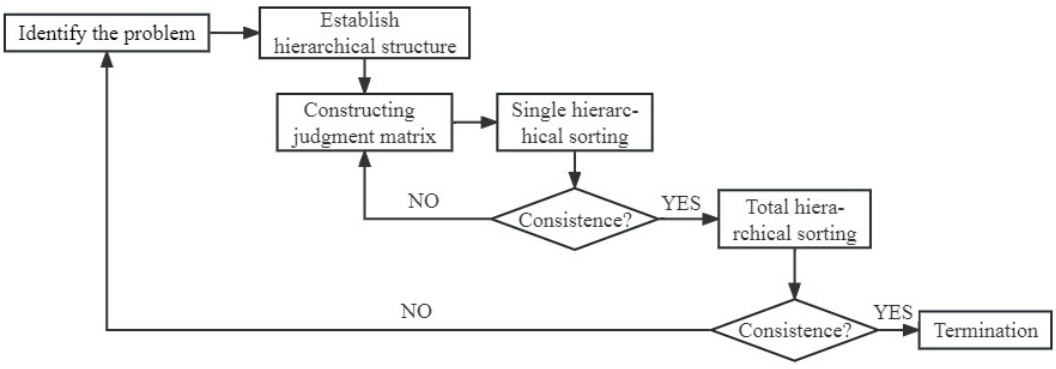

Fig. 4 The standard process of AHP

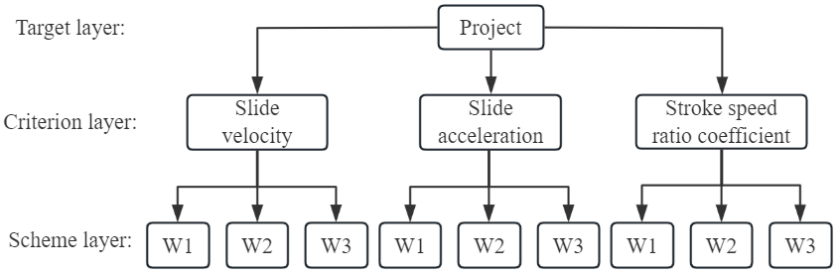

Fig. 5 The hierarchical structure model

Ten experts were invited to score the influencing factors one by one, and the scoring results of each expert were averaged. The scoring results of experts are shown in Tables 3 - 6.

Table 3

Judgment matrix formed by criterion layer and target layer

Judgment factors	Slide velocity	Slide acceleration	Stroke speed ratio coefficient
Slide velocity	1	0.5	0.33
Slide acceleration	2	1	2
Stroke speed ratio coefficient	3	0.5	1

Table 4

Judgment matrix of slider speed in scheme layer

Judgment factors	W_1	W_2	W_3
W_1	1	3	2
W_2	0.33	1	0.5
W_3	0.5	2	1

Table 5

Judgment matrix of slide acceleration in scheme layer

Judgment factors	W_1	W_2	W_3
W_1	1	0.5	0.25
W_2	2	1	2
W_3	4	0.5	1

Table 6

Judgment matrix of stroke speed ratio coefficient in scheme layer

Judgment factors	W_1	W_2	W_3
W_1	1	5	3
W_2	0.2	1	0.2
W_3	0.33	5	1

From Table 3, the feature vector is obtained as $W_c = [0.1633, 0.5393, 0.2974]$, and the maximum eigenvalue of the judgment matrix is calculated as $\lambda_{\max} = 3.0055$. After consistency check, $CI = 0.0028$, $RI = 0.52$ and $CR = \frac{CI}{RI} = 0.0054 < 0.1$ meet the requirements of consistency. Similarly, the weights of Tables 4-6 are calculated in the same way. The results in Tables 4-6 are multiplied with the results in Table 3 to obtain the total weight of the scheme layer to the target layer, as shown in Table 7.

Table7

The total weight of the scheme layer to the target layer

Criterion layer	weight	Scheme layer	weight	total weight
Slide velocity	0.1633	W_1	0.8451	0.1380
		W_2	0.1635	0.0267
		W_3	0.2970	0.0485
Slide acceleration	0.5393	W_1	0.1908	0.1029
		W_2	0.2781	0.1500
		W_3	0.4218	0.2275
Stroke speed ratio coefficient	0.2974	W_1	0.6459	0.1921
		W_2	0.1221	0.0363
		W_3	0.2286	0.0680

Finally, $W_{final} = \left[\sum W_1 \quad \sum W_2 \quad \sum W_3\right] = [0.4430 \quad 0.2130 \quad 0.3440]$.

The Final evaluation function can be obtained as follows:

$$f(X) = 0.4430 f_1(X) + 0.2130 f_2(X) + 0.3440 f_3(X) \tag{34}$$

2.4.3. Penalty function method

The use of genetic algorithms for optimization requires appropriate handling of constraints. The optimized constraint conditions include nonlinear inequalities, and the penalty function method is selected for constraint conditions. The key to the penalty function method is to construct appropriate penalty terms that can measure the degree to which the solution does not meet the constraint conditions while ensuring computational efficiency. If the selection of the penalty factor *r* is too small, the required global optimal solution cannot be obtained; if it is too large, it will reduce the efficiency. Usually, *r* is established as an increasing positive sequence to find the optimal solution that approximates the penalty function.

There are two kinds of penalty function methods: outer point method and inner point method. The outer point method is an algorithm that starts from the outside the feasible region and adds corresponding penalties to the points in the objective function that violates the constraint conditions. Points that meet the constraint conditions will not be penalized. As the iteration time increases, penalty also increases, so as to force the iteration point to approach the feasible region [19]. The outer point method in the penalty function method is used for solving.

$$F(X)=f(X)+r\sum_{j}^{15}\max\left[0,g_j(x)\right]^2 \tag{35}$$

where $F(X)$ is the penalty function; $f(X)$ is the evaluation function; r is the penalty factor; $\sum_{j}^{15}\max\left[0,g_j(x)\right]^2$ is the penalty term, and $g_j(x)$ is the constraint condition.

2.4.4. GA method

There are many intelligent optimization algorithms, such as genetic algorithm, particle swarm optimization algorithm, simulated annealing algorithm, and whale algorithm. The advantage of genetic algorithm is that it is not easy to fall into the trap of local optimal solution. The genetic algorithm is used here for solution. The parameters of genetic algorithm mainly include initial population size, crossover rate, and mutation rate. These parameters have a significant impact on the optimization results [20]. The initial population size is generally obtained from experience. The meaning of crossover rate is to participate in crossover when it is greater than the crossover rate; conversely, it will not participate in crossover. The variation rate should not be too high or too low. After comprehensive consideration, the genetic algorithm parameters are set as shown in Table 8.

Table 8

Parameters of GA

Parameters	Value
Initial population size	100
Crossover rate	80%
Variation rate	10%
Iterations	200

The optimization process of GA is shown in Figure 6.

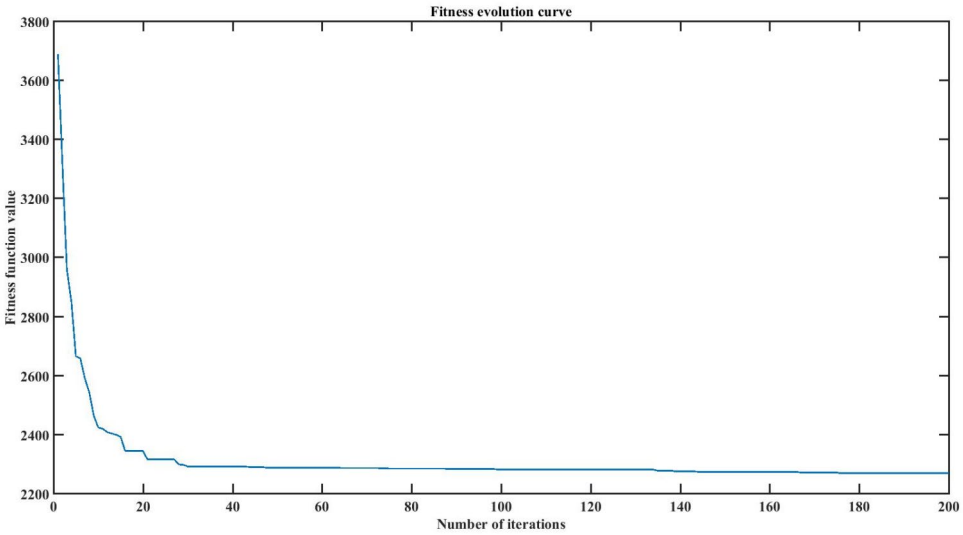

Fig. 6 The optimization process of GA

3. Results

After GA calculation, the optimized design variables are shown in Table 9.

Table 9

Comparison of parameters before and after optimization

Design variable	Before optimization	After optimization
l_1 (mm)	219.2	188
l_2 (mm)	340	342.1
l_4 (mm)	290	287.8
l_5 (mm)	430	429.2
l_3 (mm)	340	344.9
l_6 (mm)	360	365.6
x (mm)	500	493.6
y (mm)	250	258.7

The optimized crank angle slider stroke curve is shown in Figure 7, where the top dead center of the slider moves forward while the bottom dead center remains unchanged. This results in a travel speed ratio coefficient of $K = 1.44$, and meets the requirements.

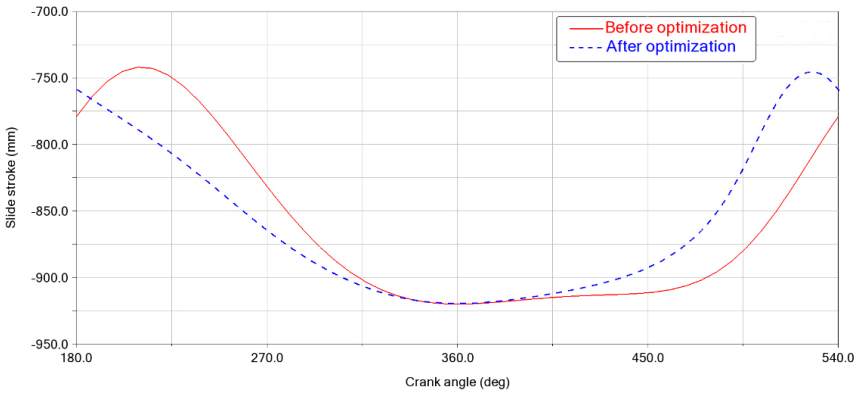

Fig. 7 Curve of the crank angle slider stroke

The optimized crank angle slider speed curve is shown in Figure 8. Within the stamping working stroke, the slider speed remains constant at 30mm/s, which meets the requirements.

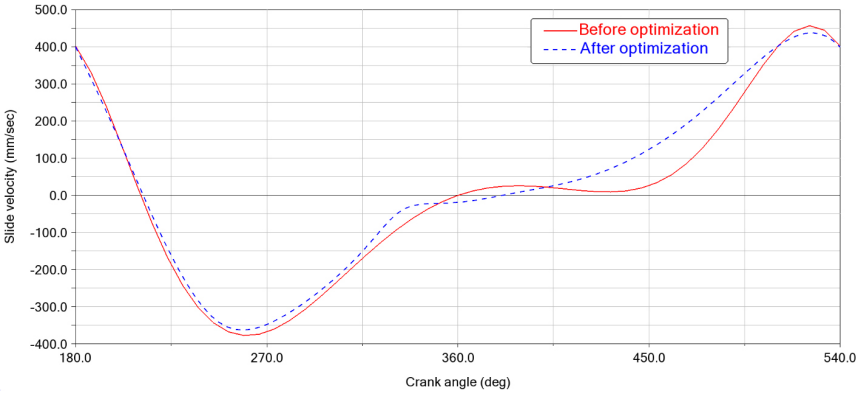

Fig. 8. Curve of crank angle slider velocity

The optimized crank angle slider acceleration curve is shown in Figure 9. Within the stamping working stroke, the slider acceleration decreases to the range of 483.6mm/s^2 to 423.4mm/s^2, which meets the requirements.

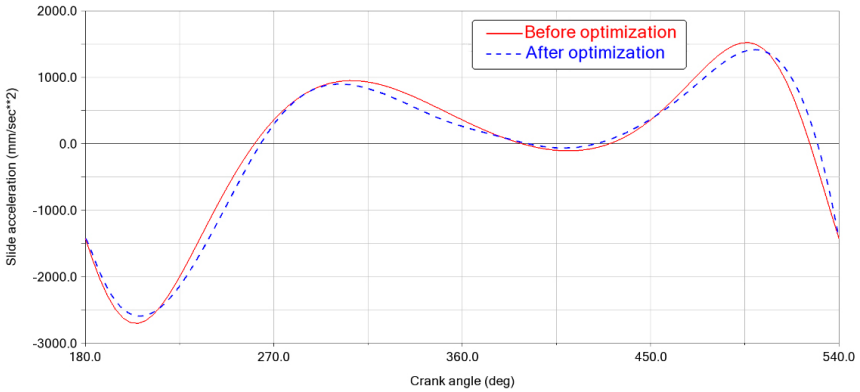

Fig. 9 Curve of the crank angle slider acceleration

4. Conclusion

(1) Using the proposed method, the slider stroke, slider speed, slider acceleration, and stroke ratio coefficient should meet the requirements proposed by enterprises.

(2) The linear weighted sum method is often used in multi-objective optimization design. However, the selection of weight coefficients is often determined by the experience of designers, which makes the design results highly subjective. Therefore, the AHP is selected to determine the weight coefficients, and can effectively meet the requirements of enterprises.

(3) In terms of optimization calculation, the GA method is used to solve the objective function. The advantage of GA is that it is not easy to fall into the trap of local optimal solution. However, the crossover rate and mutation rate need to be determined through a large number of experiments. An initial population of 100, a crossover rate of 80%, a variation rate of 10%, and an iteration count of 200 are selected. The results show that these parameters can converge to the target value fast.

Although certain results have been achieved in the crank triangular linkage-elbow mechanism of servo press, there are still shortcomings, which need to be continuously improved in future research:

(1) Only the case of uniform rotation of the servo motor is considered for kinematic analysis. In reality, the output characteristics of the servo motor are different in each stage, and the variation form is relatively complex. In the future, the output characteristics of servo motors can be combined to analyze the motion characteristics of the crank triangle elbow mechanism.

(2)The methods still need to be innovated.

(3)There are many factors that affect the performance of the crank triangular linkage-elbow mechanism in practical work, and they also have a

significant impact on the optimization results. For example, the mechanism may vibrate during motion, and it is necessary to add relevant constraint conditions to be closer to practical engineering and make the mathematical model more accurate.

Acknowledgement

This study was financially supported by General Scientific Research Projects of Zhejiang Provincial Department of Education with the project number of Y202351996.

REFERENCES

[1] *P. Groche, A. Breunig, K. Chen, D. A. Molitor, J. Ha, B. L. Kinsey and Y. P. Korkolis.* "Effectiveness of different closed-loop control strategies for deep drawing on single-acting 3D Servo Presses", CIRP Annals, **vol. 71**, no. 1, 2022, pp. 357-360. DOI:10.1016/j.cirp.2022.04.072

[2] *J. Olaizola, E. Esteban, J. Trinidad, et al.*, "Integral design and manufacturing methodology of a reduced-scale servo press", IEEE/ASME Transactions on Mechatronics, **vol. 26** no. 5, 2020, pp. 2418-2428. DOI:10.1109/TMECH.2020.3039678

[3] *R. Peón-Escalante, F. C. Jiménez, M. A. E. Soberanis, et al.*, "Path generation with dwells in the optimum dimensional synthesis of Stephenson III six-bar mechanisms", Mechanism and Machine Theory, **vol. 144**, 2020, Article ID: 103650. DOI:10.1016/j.mechmachtheory.2019.103650

[4] *A. Qaiyum and A. Mohammad*, "Optimal synthesis of six bar mechanism using particle swarm optimization", International Journal of Recent Technology and Engineering, **vol. 8**, no. 6, 2020, pp. 5287-5292. DOI: 10.35940/ijrte.F9802.038620

[5] *B. K. Belleri and S. B. Kerur*, "Balancing of planar six-bar mechanism with genetic algorithm", Journal of Mechanical and Energy Engineering, **vol. 4**, no. 4, 2020, pp. 303-308. DOI: 10.30464/jmee.2020.4.4.303

[6] *A. Reza and M. Moslehi*, "Optimal synthesis of an adjusTable six-bar path generator mechanism using a cuckoo optimization algorithm", Journal of Mechanics of Materials and Structures, **vol. 17**, no.2, 2022, pp. 149-167. DOI: 10.2140/jomms.2022.17.149

[7] *F. Sanchez-Marin and V. Roda-Casanova*, "An approach for the global search for top-quality six-bar dwell linkages", Mechanism and Machine Theory, **vol. 176**, 2022, Article ID: 104974. DOI: 10.1016/j.mechmachtheory.2022.104974

[8] *A. E. Yazdani and S. Abyaneh*, "Dimensional Synthesis of a Six-bar Shaper Mechanism with the Genetic Algorithm Optimization Approach", International Journal of Mechanical Engineering and Robotics Research, **vol. 12**, no. 2, 2023. DOI: 10.18178/ijmerr.12.2.113-120

[9] *X. Zhu, Y. Ding, X. Cai, et al.*, "Optimal schedule for agricultural machinery using an improved Immune-Tabu Search Algorithm", In 2017 36th Chinese Control Conference (CCC). IEEE, 2017: 2824-2829. DOI:10.23919/ChiCC.2017.8027793

[10] *A. R. Munoz and T. A. Lipo*, "Complex vector model of the squirrel-cage induction machine including instantaneous rotor bar currents", IEEE transactions on industry applications, **vol. 35**, no. 6, 1999, pp. 1332-1340. DOI: 10.1109/28.806047

[11] *L. Zhang, K. Hu and C. Tu*, "Design methods of planar six-bar mechanism in servo applications", Journal of the Chinese Institute of Engineers, **vol. 45**, no. 7, 2022, pp. 569-578. DOI:10.1080/02533839.2022.2101533

[12] *L. Aimin, X. Zhiyang, et al.*, "Study on Impact of Upender Based on ADAMS", 2011 Fourth International Conference on Intelligent Computation Technology and Automation. IEEE, **vol. 1**, 2011, pp. 936-939. DOI: 10.1109/ICICTA.2011.235

[13] *P. Ponomarev, I. Petrov, N. Bianchi, et al.*, "Selection of geometric design variables for fine numerical optimizations of electrical machines", IEEE Transactions on Magnetics, **vol. 51**, no. 12, 2015, pp. 1-8. DOI: 10.1109/TMAG.2015.2461682

[14] *K. Suresh, K. Shankar and C. Sujatha.*, "A four bar mechanism as dynamic magnifier for improved performance of multi-modal piezoelectric harvester beams", The European Physical Journal Special Topics, **vol. 231**, no. 8, 2022, pp. 1373-1382. DOI:10.1140/EPJS/S11734-022-00505-W

[15] *C. H. Yang and X. Shao.*, "Kinematics modeling and analysis on toggle mechanism for mechanical press", Forging & Stamping Technology, **vol. 42**, no. 12, 2017, pp.87-91.DOI:10.13330/j.issn.1000-3940.2017.12.016

[16] *D. Anh-Tuan and N. Dinh-Ngoc*, "Design Complex-Stroke Press Using Synchronous Motors", International Journal of Mechanical Engineering and Robotics Research, **vol. 12**, no. 4, 2023. DOI: 10.18178/ijmerr.12.4.249-257

[17] *R. Wang, Z. Zhou, H. Ishibuchi, et al.*, "Localized weighted sum method for many-objective optimization", IEEE Transactions on Evolutionary Computation, **vol. 22**, no. 1, 2016, pp. 3-18. DOI: 10.1109/TEVC.2016.2611642

[18] *J. E. Leal*, "AHP-express: A simplified version of the analytical hierarchy process method", MethodsX, **vol. 7**, 2020, Article ID: 100748. DOI:10.1016/j.mex.2019.11.021

[19] *A. Jayswal and M. Arana-Jiménez*, "Robust penalty function method for an uncertain multi-time control optimization problems", Journal of Mathematical Analysis and Applications, **vol. 505**, no. 1, 2022, Article ID: 125453. DOI:10.1016/j.jmaa.2021.125453

[20] *A. Del Prete and T. Primo*, "Sheet Metal Forming Optimization Methodology for Servo Press Process Control Improvement", Metals, **vol. 10**, no. 2, 2020, Article ID: 271. DOI:10.3390/met10020271